

# A description of the interaction of positrons with atoms using effective potentials

A. Zubiaga,\* F. Tuomisto, and M. J. Puska

*Department of Applied Physics, Aalto University,*

*P.O. Box 11100, FIN-00076 Aalto Espoo, Finland*

## Abstract

We have studied systems composed by a positron interacting with light atoms (H, He, Li and Be). The many-body wavefunction and the energy, including the non-adiabatic correlation, have been calculated using explicitly correlated gaussians basis functions and a stochastic variational optimization method. We discuss the interaction of positrons with atoms in a visual way by analyzing the density distributions of the light particles (electrons and positrons) and we propose an effective potential to describes the positron. The effective positron potential constructed yields the positron density and interaction energy. The scattering lengths and phase shifts obtained within the single-particle scheme are in good agreement with values from many-body calculations and the positron distributions in the bulk of Li and Be are in good agreement with density functional densities. The effective positron potential is a step forward to a robust single particle description for the positron and it can be used to describe positrons in molecular materials when it appears in the positronium form, a bound state of an electron and a positron.

---

\* asier.zubiaga@aalto.fi

## I. INTRODUCTION

The chemistry of positron, the antiparticle of the electron, in crystalline solids and soft-condensed matter has an intrinsic interest by itself but it can also be used to study the electron chemistry and the material properties depending on the open volume distribution. In crystalline solids or soft matter, thermalized positrons distribute in the open volume pockets where the repulsion by the nucleus is minimum. In soft-condensed matter positrons can bind an electron and form positronium (Ps), a leptonic "atom" with particular properties. The lifetime in vacuum of ortho-Ps, the triplet state of Ps (o-Ps), is long, 142 ns, because it annihilates via the "slow" emission of three gamma photons. When inside the matter a positron and an o-Ps annihilates through pick-off processes with electrons of the matter. It is a "fast" process where typically two gamma photons are emitted [1].

The gamma photons coming from the pick-off annihilation contain valuable information about the local electronic structure of the material. The lifetime of positrons in metals and semiconductors can be used to identify the annihilation site, perfect bulk lattice, an atom monovacancy or a cluster of vacancies [2]. The lifetime spectroscopy of o-Ps has a rather unique role as a method capable to study properties related with the open volume in molecular materials. The size distributions and densities of nanometre-sized voids can be measured in porous SiO<sub>2</sub> [3, 4], polymers [5] and biostructures [6]. More recently, phase transitions in polymers [7] and biostructures [8] have also been studied.

Both the electron and the positron are light quantum-mechanical particles and a full quantum-mechanical description is needed to address the non-adiabatic correlation effects. Quantum mechanical effects such as delocalization or the zero-point energy play a big role also. Regrettably, a full quantum-mechanical treatment of the interacting electron-positron system embedded in a host material is clearly beyond the present-day computational capacity.

The density distributions and the annihilation properties of positrons in metals and semiconductors can be calculated to a good accuracy within the Density Functional Theory (DFT). Calculated values of the positron annihilation parameters can be used for a quantitative analysis of the experimental results [9]. For a quantitative analysis of Ps in molecular materials one should be able to model o-Ps states and annihilation with a predictive power. The semi-empirical models [10] provide an estimation of the size of the open volume pocket

where Ps annihilates but it cannot be applied to open volume pockets distributed arbitrarily and it does not address the chemical specificity of the material in a consistent way.

The wavefunctions of small systems composed by a positron interacting with a light atom or a small molecule can be calculated using accurate many-body techniques. Quantum Monte-Carlo (QMC) has been used to study positron binding to hydrogen cyanide, alkali-metal hydrides [11] and Ps complexes with atoms and ions [12]. Configuration Interaction (CI) has been used to study interactions of positrons with alkali monoxides [13]. The Stochastic Variational Method (SVM) together with Explicitly Correlated Gaussian (ECG) function basis [14, 15] (ECG-SVM) has been applied to positronic Li [16] and positronic Be[17].

Gaussian correlation functions describe accurately the inter-particle correlations and they are better suited for the description of positronic systems than atomic and molecular orbitals. The energy values of ECG-SVM wavefunctions are lower than those of the CI calculations for systems involving a positron or positronium [15]. In the present study ECG-SVM has been used to calculate accurate energies and wavefunctions for several complexes comprising a positron and a light atom (H, He, Li and Be). The electron and positron density distributions and the effective positron potential provide a clear way for the visualization of the interacting atom-positron many-body system. The knowledge gained in this study allow us to propose an effective potential to describe the interaction of a positron with matter. Thereby we pave the way toward an efficient scheme capable to predict the positron and, especially, Ps annihilation characteristics in molecular materials.

## II. COMPUTATIONAL METHODS

We have used all-particle ab-initio calculations to calculate the many-body wavefunction and energy of a positron interacting with a light atom. We have also calculated the total energy of the neutral atoms and the positive ions to determine the ionization energies. We considered the hadronic nucleus as a particle without structure, in equal footing of the electrons and the positron. The wavefunction is expanded in terms of a linear combination of properly antisymmetrized explicitly correlated Gaussian (ECG) [14] functions

$$\Psi = \sum_{i=1}^s c_i \psi_{SMs}^i(\vec{x}, A^i) = \sum_{i=1}^s c_i \mathcal{A} \left\{ \exp \left( -\frac{1}{2} \sum_{\mu, \nu=1}^{N-1} A_{\mu\nu}^i \vec{x}_\mu \vec{x}_\nu \right) \otimes \chi_{SMs} \right\}, \quad (1)$$

where  $A_{\mu\nu}^i$  are the non-linear coefficients of the gaussians and  $c_i$  the linear mixing coefficients of the eigenvectors of the diagonalized Hamiltonian.  $\mathcal{A}$  is an antisymmetrization operator that acts on indistinguishable particles.  $\chi_{SMs}$  is a spin eigenfunction with  $\hat{S}^2\chi_{SMs} = S(S+1)\hbar^2\chi_{SMs}$  and  $\hat{S}_z\chi_{SMs} = M_S\hbar\chi_{SMs}$ . The ECG wavefunction uses Jacobi coordinate sets  $\{\vec{x}_1, \dots, \vec{x}_{N-1}\}$  with the reduced mass  $\mu_i = m_{i+1} \sum_{j=1}^i m_j / \sum_{j=1}^{i+1} m_j$  that allows for a straightforward separation of the CM movement. In a general case, the wavefunction needs to include also spherical harmonics to describe orbital motion, but all the systems we have considered so far have zero total angular momentum.

The wavefunctions are eigenstates of the non-relativistic Hamiltonian without the kinetic energy of the center-of-mass ( $T_{CM}$ )

$$\hat{H} = \sum_i \frac{p_i^2}{2m_i} - T_{CM} + \sum_{i<j} \frac{q_i q_j}{4\pi\epsilon_0 r_{ij}}, \quad (2)$$

where  $\vec{p}_i$  are the momenta,  $m_i$  the masses, and  $q_i$  the charges.  $r_{ij}$  is the distance between the  $i^{\text{th}}$  and  $j^{\text{th}}$  particles. The ECG basis comprises in our calculations between 200 and 2000 functions. Typically, systems with more particles need larger function bases for an accurate determination of the wavefunction.

The nonlinear coefficients  $A_{\mu\nu}^i$  need to be optimized to avoid very large ECG bases. A stochastic variational method (SVM) has been used to optimize the bases instead of a direct search method, because it is better suited to functions with a large number of parameters. The values of the parameters are generated randomly and they are kept only if the update lowers the total energy of the system. The algorithms and the computer capacity available nowadays allows to treat systems with up to eight particles. The ECG-SVM method has been successful because the matrix elements involving ECG functions are computed analytically in an efficient manner.

To calculate unbound interacting systems, we have added a two-body attractive potential that binds the positron to the hadronic nucleus. The potential is different from zero only when the distance grows above a boundary value, and then it has a parabolic increase. The variational principle applies to the modified Hamiltonian and the optimization is more robust than in a previous method based in modifying the boundaries of the non-linear parameters [18]. If the confinement radius is chosen large enough, the shape of the wavefunction is not affected in the interaction region by the details of the confinement. The contribution of the confinement potential to the total energy is small and it can be subtracted from the

total energy when determining the interaction potential.

The virial coefficient is defined as  $2 \langle T \rangle / \langle V \rangle + 1$  where  $\langle T \rangle$  and  $\langle V \rangle$  are the expectation values of the kinetic energy and the potential energy, respectively. It is zero for the exact wavefunction of a particle system interacting only through the Coulomb interaction. Non-zero values measure the quality of the wavefunction. In confined systems with a non-Coulombic external potential it will be non-zero. When the confinement radius is large enough the effect of the confinement potential is negligible and the deviation of the virial coefficient from zero measures mainly the quality of the wavefunction. Low values of the virial coefficient allow to calculate accurate electron and positron densities from the wavefunction.

### III. ECG CALCULATIONS

A positron forms a bound state with Li and Be atoms (Li-e<sup>+</sup> and Be-e<sup>+</sup>) and it remains unbound when interacting with H and He (H-e<sup>+</sup> and He-e<sup>+</sup>). We define the asymptotic state when the nucleus and the positron are separated to a distance where they don't interact anymore. Unbound systems and Be-e<sup>+</sup> will split into a neutral atom and a positron but the bound positronic Li split into a Li<sup>+</sup> ion and a Ps atom, instead. We call to the difference of the energy of the interacting system,  $E_{Xe^+}$ , and the isolated atom,  $E_X$ , as the positron interaction energy  $E_{int}^{e^+} = E_{Xe^+} - E_X$ . The Ps interaction energy,  $E_{int}^{Ps} = E_{Xe^+} - E_{X^+} - E_{Ps}$ , is the difference between the total energy of the interacting system and the sum of total energies of the positive ion,  $E_{X^+}$ , and Ps,  $E_{Ps}$ . Only for bound states are both interaction energies negative. The value is larger (positive or negative) for the main dissociation channel. Only the main dissociation channel is given in table I.

We have used a potential well with a large radius (100 au) to calculate the positronic H and He. The resulting mean positron distance is large and the interaction energy small. The basis size used to describe positronic H is 200, enough to get a well converged energy. The virial coefficient is  $5 \times 10^{-4}$ . The basis for the positronic He has 1000 functions and the virial coefficient is  $1 \times 10^{-4}$ . The ionization energies of H and He are 0.5 au and 0.90369 au, respectively, well above the binding energy of Ps (0.25 au). The electron densities of the interacting H and He, upper left and right panels of figure 1, respectively, do not show an appreciable polarization. The positron density in both systems is completely delocalized

Table I. Size of the function basis, total energy of the system and value of the virial coefficient for all the calculated positronic systems. The positron mean distance to the nucleus ( $\langle r_p \rangle$ ) and the interaction energy for the main dissociation channel  $E_{int}$  are also given. The main dissociation channels are labeled as  $e^+$ , when the asymptotic state includes a positron, and Ps, when the asymptotic state includes a Ps atom. The values of  $E_{int}$  in parentheses are the best values from the literature. All values are given in atomic units, except for the virial coefficient that is dimensionless.

System	Basis size	Energy	virial	$\langle r_p \rangle$	Channel	$E_{int}$
H- $e^+$	200	-0.49974	$5 \times 10^{-4}$	67.47	$e^+$	0.262E-3
He- $e^+$	1000	-2.90332	$1 \times 10^{-4}$	56.98	$e^+$	0.372E-3
Li- $e^+$	1000	-7.53226	$7 \times 10^{-6}$	9.928	Ps	-2.42E-3
				(9.9376 [16])		(-2.4821E-3 [16])
Be- $e^+$	2000	-14.6694	$6 \times 10^{-5}$	10.972	$e^+$	-2.01E-3
				(9.9105 [17])		(-3.163E-3 [17])

and only a small fraction of the density penetrates the electron cloud of the atom.

Using ECG-SVM, the positronic Li [16] and Be [17] have been shown to form bound states. The best values obtained for their binding energy are  $2.4821 \times 10^{-3}$  au and  $3.163 \times 10^{-3}$  au, respectively. In our calculations we have used a basis with 1000 functions to calculate the positronic Li and 2000 functions for the positronic Be. For Li this basis results in a binding energy of  $2.42 \times 10^{-3}$  au, close to the reference value. The Ps binding energy is larger than the ionization energy, 0.19814 au, and the positron can form a Ps cluster with the 2s electron of Li. This is clearly seen in the electron density distribution shown in the lower left panel of figure 1. The positronic Be is a large system with a small binding energy, which is difficult to optimize. The calculated binding energy is  $2.01 \times 10^{-3}$  au while the best value from the literature is  $3.163 \times 10^{-3}$  au. The 2s orbital is closed and its ionization energy is larger (0.34242 au) than the binding energy of Ps. This prevents the electron density from being polarized and form a Ps cluster (see the lower right panel of figure 1). The positron is bound by the dipole induced in the electron cloud of Be, instead. Because the binding energies are small the positron lies far from the nucleus. For Li- $e^+$  and Be- $e^+$ , the mean positron distance are 9.928 au and 10.972 au, respectively. The virial coefficient for the positronic Li

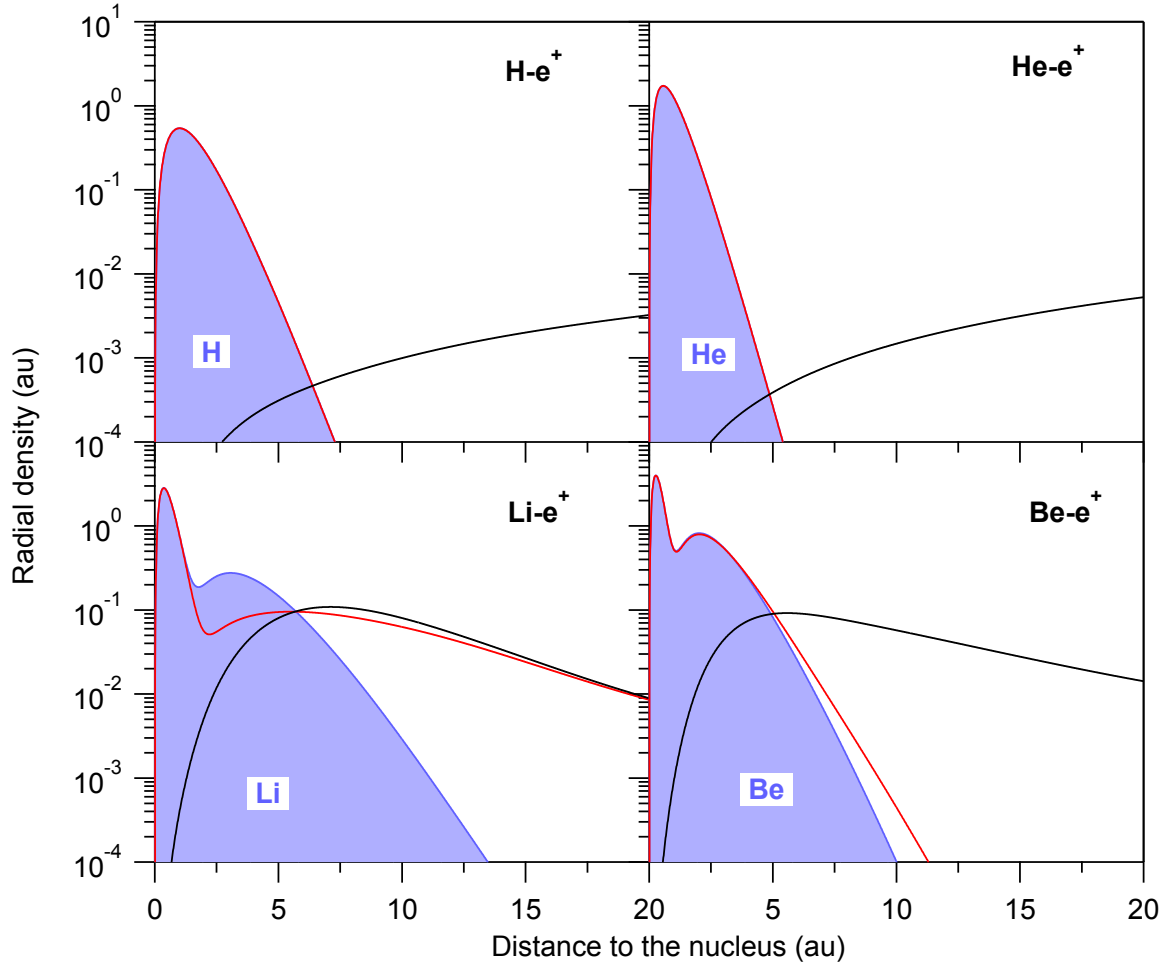


Figure 1. (Color online) Electron densities in the isolated atoms (filled blue curve), and in the interacting positron-atom systems (red curve), as well as the positron density (black curve) in the latter systems. The upper panels show the  $\text{H-e}^+$  (left panel) and the  $\text{He-e}^+$  (right panel) unbound systems. The lower panels show the positronic Li (left panel) and the positronic Be (right panel) bound complexes.

is  $7 \times 10^{-6}$  while for the positronic Be it is  $6 \times 10^{-5}$ .

#### IV. EFFECTIVE POTENTIALS

We define an effective potential ( $V_{eff}$ ) using the positron densities ( $\rho$ ) of the interacting systems. For that purpose, the Schrödinger equation has been inverted using an effective

energy  $E_{eff}$  and an effective mass  $M_{eff}$

$$V_{eff}(r) = E_{eff} + \frac{1}{2M_{eff}} \frac{\nabla^2 \sqrt{\rho}}{\sqrt{\rho}}. \quad (3)$$

The potential is constructed so that it vanishes when the positron lies at a long distance from the atom. For systems dissociating into a positron and a neutral atom (H-e<sup>+</sup>, He-e<sup>+</sup> and Be-e<sup>+</sup>),  $E_{eff}^{e^+}$  is the positron interaction energy and  $M_{eff}^{e^+}$  is the mass of the positron. For systems where the asymptotic state includes a Ps cluster (Li-e<sup>+</sup>),  $E_{eff}^{Ps}$  is the Ps-ion interaction energy and the effective mass is  $M_{eff}^{Ps} = 2m_e$ . Only for the right combination of  $E_{eff}$  and  $M_{eff}$  has  $V_{eff}$  the correct behaviour at large separations. When the main dissociation channel includes Ps (a positron), the asymptotic values of  $V_{eff}^{e^+}$  ( $V_{eff}^{Ps}$ ) is negative and equal to the difference between the ionization energy of the neutral atom and the binding energy of Ps.

The upper left panel of figure 2 shows the  $V_{eff}^{e^+}$  and the  $V_{eff}^{Ps}$  for H-e<sup>+</sup>. Because the system dissociates to the H atom and the positron,  $V_{eff}^{e^+}$  has the correct asymptotic behavior and  $V_{eff}^{Ps}$  is negative and finite (-0.25 au). Also the  $V_{eff}^{e^+}$  of unbound He-e<sup>+</sup>, shown in the upper right panel of figure 2, has the correct asymptotic behavior while the  $V_{eff}^{Ps}$  is 0.654 au below zero. The potentials of both atoms have a strongly repulsive core at distances to the nucleus lower than 1.2-1.3 au and a shallow potential well in the interaction region that extends to 5 au for H-e<sup>+</sup> and to 3.7 au for He-e<sup>+</sup>. However, the weak attractive well, induced by the polarization of the electron cloud by the positron, does not bind the positron. The longer range of the attractive interaction region of H-e<sup>+</sup> agrees with the larger polarizability of H.

Li-e<sup>+</sup> dissociates by transferring the 2s electron to the Ps. Accordingly,  $V_{eff}^{Ps}$  is well defined and  $E_{eff}^{Ps}$  is the negative binding energy against dissociation into Li<sup>+</sup> and Ps. On the other side, the asymptotic value of  $V_{eff}^{e^+}$  is 0.0542 au below zero. The potential has a strongly repulsive core at separations shorter than 3 au. It extends to a longer distance than that in H and He because the 2s electron of Li contributes to it. The minimum value of the potential well is  $-24.57 \times 10^{-3}$  au at a separation of 4.62 au. On the other side, Be-e<sup>+</sup> dissociates to neutral Be and a positron. The bare positron effective potential (see lower right panel of figure 2) has the correct asymptotic behaviour and  $V_{eff}^{Ps}$  is 0.0947 au below zero. The electron cloud of Be is more compact than Li and the repulsive cores starts at 2.14 au. The potential well is  $-84.58 \times 10^{-3}$  au deep at 3.18 au.

As will be shown below, the effective potentials can be used to calculate the density



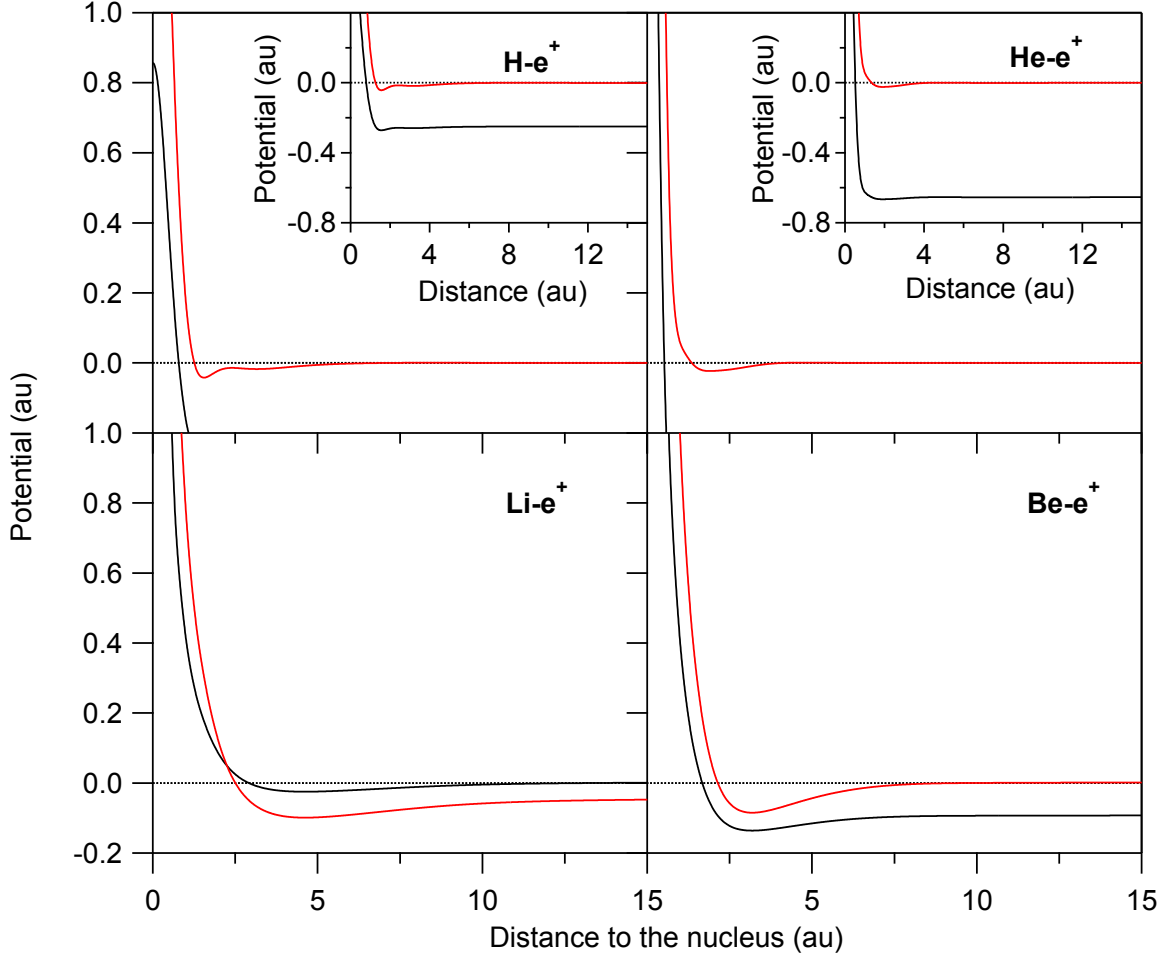


Figure 2. (Color online) Effective potentials for unbound  $\text{H-e}^+$  (upper left panel), unbound  $\text{He-e}^+$  (upper right panel), positronic Li complex (lower left panel) and positronic Be complex (lower right panel). Black curves correspond to the positronium effective potential and red curves to the bare positron effective potential.

distribution and the binding energies of the positron.  $V_{eff}^{Ps}$  describes a positron within a Ps cluster. The interaction with the electron in Ps is implicit in the potential. A mass normalized definition of  $V_{eff}^{Ps}$  can be given as  $V_{eff'}^{Ps} = M_{eff} E_{int}^{Ps} + \nabla^2 \sqrt{\rho}/2\sqrt{\rho}$ . In this work, we favor the definition in equation 3 because it allows a straight comparison with the many-body interaction energies. Both definitions yield the same positron density. We have used the mass normalized effective potential in section VIB to compare the  $V_{eff}^{Ps}$  with the DFT potentials.

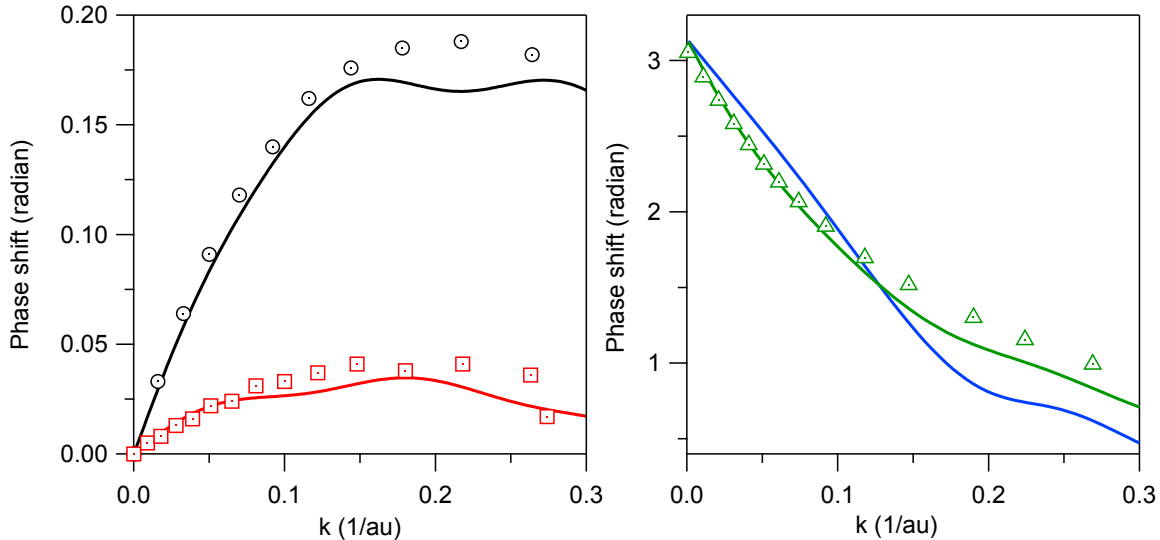


Figure 3. (Color online) s-wave phase shifts of positrons scattering off H (black line), He (red line), Li (blue line) and Be (green line). The many body values obtained by Zhang et al. [19] for H (black dotted circles) and He (red dotted squares) and Bromley et al. [20] for Be (green dotted triangles) are also shown.

## V. SCATTERING LENGTH

Zhang et al. [19] calculated the positron s-wave phase shifts ( $\delta_0$ ) and the scattering lengths ( $a_0$ ) for H and He using ECG-SVM and stabilization techniques. Houston et al. [21] used Hylleraas wavefunctions and the Kohn variational method to calculate  $a_0$  for H. Bromley et al. [20] calculated for Be  $\delta_0$  and  $a_0$  using polarized orbital wavefunctions. We have calculated  $\delta_0$  and  $a_0$  from  $V_{eff}$  from the s-wave scattering wavefunction  $\psi_0$ . The s-wave scattering wavefunction for a positron of energy  $E = k^2/2M_{eff}$  is calculated by solving the radial Schrödinger equation. The effective mass is  $m_e$  for all studied cases except for Li- $e^+$  for which it is  $2m_e$ . At large distances from the nucleus the solution has the form

$$\lim_{r \rightarrow \infty} \psi_0 = \frac{\sin(kr + \delta_0)}{kr}. \quad (4)$$

The wavefunction is fitted to this asymptotic to obtain the phase shift as a function of  $k$  and  $a_0$  is calculated at the low energy limit from  $k \cot \delta_0 = -1/a_0 + O(k^2)$ . In potentials with an attractive well, like  $V_{eff}$ , the scattering length will be negative when there is not a bound state.

The phase shifts  $\delta_0$  show a good agreement with the many-body values (see figure 3) for  $k < 0.1 \text{ au}^{-1}$  and for larger momenta the agreement degrades slightly. The interaction energies of H-e<sup>+</sup> and He-e<sup>+</sup> where the  $V_{eff}^+$  have been derived from are  $0.262 \times 10^{-3} \text{ au}$  and  $0.272 \times 10^{-3} \text{ au}$ , respectively, while for  $k > 0.1 \text{ au}^{-1}$   $E > 5 \times 10^{-3} \text{ au}$ . The missing dynamical correlation effects are responsible for the deviation from the many-body result. For Be the agreement between both phase shifts is also good for  $k < 0.1 \text{ au}^{-1}$  even if  $V_{eff}^+$  describes a bound state.

Table II. Positron scattering lengths computed from  $V_{eff}$  and the Coulomb potentials of the nucleus and the electrons. The values of  $V_{Coul}$  have been obtained using the electron density of the isolated atom ( $V_{Coul}^X$ ) and the interacting system ( $V_{Coul}^{X-e^+}$ ). The values in the last column are reference values from the literature. All the values are given in au.

	$V_{eff}$	$V_{Coul}^X$	$V_{Coul}^{X-e^+}$	
H-e <sup>+</sup>	-1.86	0.58	0.58	-2.094 [19], -2.10278 [21]
He-e <sup>+</sup>	-0.55	0.43	0.43	-0.474 [19]
Be-e <sup>+</sup>	18.76	1.58	1.69	16 [20]
Li-e <sup>+</sup>	12.19	2.08	8.32	-

The deviation of the scattering lengths (see table II) of the  $V_{eff}^+$  for H and He is less than 12% and it is 16% for Be. The positron scattering length for Li is around 2/3 of that for Be. There are no reference values for the positron scattering length for Li available in the literature but many-body calculations of the scattering cross section [22, 23] show that the polarization of the target atom and the formation of Ps are important already at low energies. To evaluate their influence in  $V_{eff}^{Ps}$ , we have checked that the static  $a_0$  is only 2.08 au (see table II). The static  $a_0$  has been calculated setting  $M_{eff} = m_e$  and using the positron Coulomb potential due to the nucleus and the electrons ( $V_{Coul}^{e^+}$ ). Using the  $V_{Coul}^{e^+}$  of the Li-e<sup>+</sup> system, the short range Coulomb repulsion of the interacting system is included and the scattering length increases to 8.32 au. The positron scattering length for the Coulomb potentials of H, He and Be have also smaller absolute value than the corresponding  $V_{eff}$ , but for the rest of the atoms  $V_{Coul}^X$  and  $V_{Coul}^{X-e^+}$  have similar scattering length. The electron-positron correlations have a large effect in the scattering properties even at low energies.

## VI. BOUND STATES: Li-e<sup>+</sup> AND Be-e<sup>+</sup>

The binding energy of the positron to Li and Be has been calculated using the corresponding  $V_{eff}$  by solving numerically the radial single-particle Schrödinger equation. In the ground state both systems have zero angular momentum and the equivalent one-dimension problem is

$$-\frac{1}{2M_{eff}}\frac{d^2U}{dr^2} + V_{eff}U = EU, \quad (5)$$

where  $U = r\Psi$  and  $\Psi$  is the s-type radial wavefunction. The boundary conditions for  $U$  are  $U(r = 0) = 0$  and  $U(r \rightarrow \infty) = 0$ . The binding energy and the mean positron distance obtained using the  $V_{eff}$  should match the ECG values by construction. For Li the calculated binding energy is  $2.414 \times 10^{-3}$  au and  $\langle r_p \rangle$  10.213 au, close to the values of the many-body calculations,  $2.42 \times 10^{-3}$  au and 9.928 au, respectively. For Be also, the agreement is good. The calculated binding energy and  $\langle r_p \rangle$  are  $2.011 \times 10^{-3}$  au and 11.104 au, respectively, and the many-body calculations yield  $E_b = 2.01 \times 10^{-3}$  au and  $\langle r_p \rangle = 10.972$  au.

### A. Atomic potentials

The positron potential has been calculated within the local density approximation (LDA) of DFT as  $V^{BN}(r) = V_{Coul}^{e+}(r) + V_{corr}^{e-p}[n_-(r)]$  where  $V_{corr}^{e-p}[n_-(r)]$  is the electron-positron correlation potential parametrized by Boronski and Nieminen [24]. We have plotted  $V^{BN}$  for Li and Be atoms in figure 4. For comparison,  $V_{Coul}^{e+}$  and the  $V_{eff}$  are also shown in each case. For Li the mass normalized  $V_{eff}^{Ps}$  is given for a direct comparison with  $V^{BN}$  and  $V_{Coul}^{e+}$ .

$V_{eff}$  shows a good agreement with  $V^{BN}$  and  $V_{Coul}^{e+}$  of Li and Be at small separations. At these distances  $V_{corr}^{e-p}$  is small compared to  $V_{Coul}^{e+}$ . At separations larger than 1.9 au  $V^{BN}$  is attractive and it tends to -0.262 au when the electron density is very low. It is more negative than  $V_{eff}$  in this range and it decreases smoothly. On the other side,  $V_{Coul}^{e+}$  always remains repulsive. The BN  $V_{corr}^{e-p}$  was parametrized from the correlation energy of a positron in a homogeneous electron gas and it tends to the Ps limit when the electron density is very low.  $V^{BN}$  shifted by 0.262 au (now zero at long separations, see the broken line of figure 4) remains positive within the whole distance range. For Li and for separations larger than 1.6 au the shifted  $V^{BN}$  is more repulsive than the mass normalized  $V_{eff}^{Ps}$ , but it is more attractive at shorter separations. For Be, the shifted  $V^{BN}$  is more repulsive than  $V_{eff}^{e+}$  in the

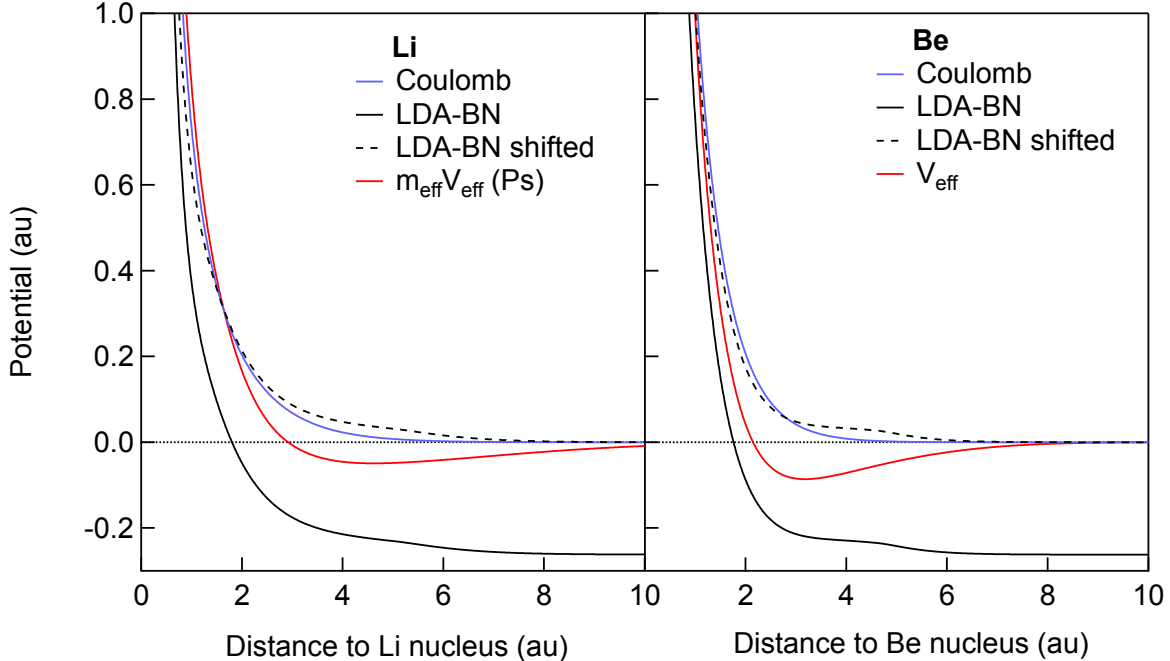


Figure 4. (Color online) Atom potentials for Li and Be. Pure Coulomb potential (blue line), LDA (black line) and the effective potential (red line). The LDA-BN potential shifted 0.262 au is also shown (black broken line) for a better comparison to the other potentials.

whole range, but both converge close to the nucleus.

## B. Solids

Li crystallizes in a body centered cubic structure with a lattice parameter of 6.59 au and Be has a face centered cubic structure and a lattice parameter of 6.04 au. The positron density and ground state energy in the solid has been obtained by solving the Schrödinger equation in a three-dimensional mesh using a numerical relaxation technique [25]. The positron potential in solids ( $V_{solid}^+$ ) can be rather reliably calculated within LDA summing the  $V_{corr}^{e-p}[n(r)]$  of the total electron density  $n(r)$  to the superposition of atomic  $V_{Coul}^{e+}$ , where  $n(r)$  is the superposition of the atomic electron densities. We have also used  $V_{eff}$  to calculate the potential of the positron in solid Li and Be as the superposition of the atomic  $V_{eff}$ . For  $V_{eff}^{Ps}$  of Li the positron effective mass has been set to  $2m_e$  in the Schrödinger equation.

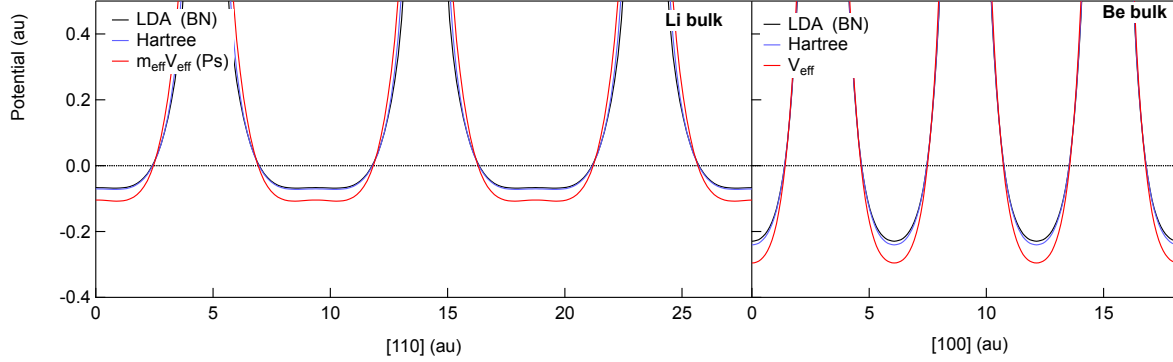


Figure 5. (Color online) Mass normalized positron potentials in solid Li along the [110] direction (left panel) and in solid Be along the [100] direction (right panel).

The positron annihilation rate ( $\lambda$ ) is

$$\lambda = \pi r_0^2 c \int \rho_+(\vec{r}) \rho_-(\vec{r}) g_0^{BN}(\rho_-(\vec{r})) d\vec{r}, \quad (6)$$

where  $r_0$  is the electron classical radius,  $c$  the speed of light,  $\rho_+$  and  $\rho_-$  are the positron and electron densities and  $g_0^{BN}(\rho_-(\vec{r}))$  is the electron-positron contact density parametrized by Boroński and Nieminen [24]. The error introduced calculating the lifetime of positrons using non-self-consistent electron densities is small because the lifetime is an integral quantity over the whole solid and the positron density relaxes following the changes of the electron density [9]. The total electron density is the superposition of ECG-SVM atomic densities in all cases.

The lower panels of figure 5 show the positron potentials in the bulk of Li and Be along the [110] and the [100] axes, respectively. The potentials have been aligned so that the zero corresponds to the positron energy eigenvalue in all cases. The mass normalized  $V_{eff}^{Ps}$  of Li is slightly more repulsive near the atom core than  $V_{Coul}^+$  and  $V^{BN}$ . In this range the effect of the  $V_{corr}^{e-p}$  is relatively small and  $V^{BN}$  is similar to  $V_{Coul}^+$ . In the interstitial region  $V_{eff}$  is more attractive than  $V^{BN}$  and  $V_{Coul}^+$ . A similar behaviour was noticed when comparing the shifted  $V^{BN}$  of a single atom to the corresponding  $V_{Coul}^+$  and  $V_{eff}$ .

According to the LDA calculation within the atomic superposition method, the positron lifetime in Li is 299 ps (see table III) and without  $V_{corr}^{e-p}$  the lifetime increases slightly to 302 ps. The value obtained using the  $V_{eff}^{Ps}$  is 8 ps longer, in good agreement with the LDA value. The positron lifetime in the bulk of Be calculated with the effective potential is 137 ps

and it agrees with the LDA value. Also  $V_{Coul}^{e^+}$ , without  $V_{corr}^{e-p}$ , gives the same lifetime value. The minimum of the mass normalized bulk potential for Li is -0.10 au below the positron energy eigenvalue while for LDA the minimum is -0.067 au below the corresponding positron eigenvalue. This difference is responsible for the slightly stronger localization of the positron in the interstitial region when  $V_{eff}^{Ps}$  is employed. In Be the difference is larger (-0.23 au for  $V^{BN}$  and -0.30 au for  $V_{eff}^{e^+}$ ). However, the much shorter lifetime of 137 ps is not affected when different approximations are used for the potential.

Table III. Positron lifetime in solid Li and Be for the three potentials discussed in the text. The lifetime values are given in ps.

	Li	Be
$V^{BN}$	299	137
$V_{Coul}^{e^+}$	302	137
$V_{eff}$	306	137

## VII. DISCUSSION

$V_{eff}^{e^+}$  and  $V_{eff}^{Ps}$  are, in both cases, a single-particle interaction potential of the positron that describes the many-body correlations accurately. They describe accurately the Coulomb interaction and the low energy correlations for a positron interacting with a single atom. The resulting low energy positron scattering properties of single atoms are comparable to many-body values. It yields good results also for positron states in bulk Li and Be where the repulsive Coulomb potential dominates, but it fails to describe the trapping of positrons at vacancies. The total effective potential describes the electron-positron correlations in terms of the correlations in atoms and it shows an attractive well due to the polarization of the electron cloud. The resulting potential is higher inside the vacancy than in the bulk. But in metals the valence electrons of all atoms form a band of delocalized states and the electron density is non-zero inside the vacancy. The electron-positron correlation lowers the positron energy inside the vacancy compared to the bulk.

$V_{eff}^{Ps}$  includes the Coulomb and correlation potentials for the electron forming the Ps, so it can yield the ground state distribution of a positron forming Ps within a single particle

approach.  $V_{eff}^{Ps}$  differs from previous description of Ps in that the distribution of the accompanying electron is implicit in the potential. It also shows the particularity that  $M_{eff} = 2m_e$ . When this is a problem, the mass normalized potential can be used instead to calculate the positron density at the expense of multiplying by a factor of 2 the positron energies. On the other side, it shows two clear advantages: a) the definition of  $V_{eff}^{Ps}$  circumvents the difficulty of defining the center of mass of Ps in a system with several electrons and b) from the positron density calculated from  $V_{eff}^{Ps}$  it is straightforward to calculate the pick-off annihilation of o-Ps with the surrounding matter [18]. This advantages are relevant specially when Ps is embedded in soft condensed matter, like polymers or biostructures, where Ps can be strongly polarized.

The  $V_{eff}^{Ps}$  of Li-e<sup>+</sup> describes the bound state of a Ps cluster with a Li<sup>+</sup> ion and it has limited applicability beyond the interaction of a single positron with gases. ECG-SVM calculations of unbound HePs show that the interaction of the positron with the surrounding matter is screened by the electron bound to it and the Pauli repulsion prevents Ps from forming a bound state [18]. When defined for unbound positronic systems including Ps, like HePs,  $V_{eff}^{Ps}$  can be very useful to study the interaction of Ps with molecular matter. In addition,  $V_{eff}^{Ps}$  can be also used to calculate the total potential in an atom model of soft molecular material and calculate the positron density and pick-off annihilation rate from equation 6. A  $V_{eff}^{Ps}$  defined in this way would allow to describe Ps in different materials and in arbitrary geometries. A full study of Ps interacting with atoms and its properties will be given in a subsequent work [26].

## VIII. CONCLUSIONS

We have calculated the energy and wavefunction for a positron interacting with light atoms using many-body ECG-SVM. We have discussed the atom-positron interactions using the densities of the electrons and the positron and we have defined an effective positron potential using the positron density. The effective potential is a mean field description of the positron in its ground state and it can be defined when the positron forms Ps. It includes the full electron-positron correlation and the electron-electron exchange with all the electrons and the charge screening. The potential describes correctly the positron distribution and the interaction energy of bound positronic Li and Be and the scattering length are consistent



with the many-body results. We also calculate the positron distribution in metallic Li and Be. The single particle effective potential describes correctly the distribution in the bulk but not in the vacancy, where the electron-positron correlations of the metal differ from the atom-positron system. Further studies of unbound Ps interacting with matter are promising to derive a  $V_{eff}^{Ps}$  that can describe self-trapped Ps in soft-molecular matter. The final goal is to define an effective single particle potential for an arbitrary material and to use it to calculate the Ps distribution in atom models of molecular materials with arbitrary geometry.

## ACKNOWLEDGMENTS

This work was supported by the Academy of Finland through the individual fellowships and the centre of excellence program. We acknowledge the computational resources provided by Aalto Science-IT project. Thanks are due to K. Varga for providing us the ECG-SVM code used in this work.

- 
- [1] O. E. Mogensen, in *Positron Annihilation in Chemistry*, Springer Series in Chemical Physics, Vol. 58, edited by H. K. V. Lotsch (Springer-Verlag, 1995).
  - [2] F. Tuomisto and I. Makkonen, “Defect identification in semiconductors: Experiment and theory of positron annihilation,” (2013), submitted to *Rev. Mod. Phys.*
  - [3] Y. Nagai, Y. Nagashima, and T. Hyodo, *Phys. Rev. B* **60**, 7677 (1999).
  - [4] L. Liskay, C. Corbel, P. Perez, P. Desgardin, M.-F. Barthe, T. Ohdaira, R. Suzuki, P. Crivelli, U. Gendotti, A. Rubbia, M. Etienne, and A. Walcarius, *Appl. Phys. Lett.* **92**, 063114 (2008).
  - [5] A. Uedono, R. Suzuki, T. Ohdaira, T. Uozumi, M. Ban, M. Kyoto, S. Tanigawa, and T. Mikado, *J. Polym. Sci. Part B* **36**, 2597 (1998).
  - [6] A. W. Dong, C. Pascual-Izarra, S. J. Pas, A. J. Hill, B. J. Boyd, and C. J. Drummond, *J. Phys. Chem. B* **113**, 84 (2009).
  - [7] C. L. Want, T. Hirade, F. H. Maurer, M. Eldrup, and N. J. Pedersen, *J. Chem. Phys.* **108**, 4654 (1998).
  - [8] P. Sane, E. Salonen, E. Falck, J. Repakova, F. Tuomisto, J. Holopainen, and I. Vattulainen, *J. Phys. Chem. B letters* **113**, 1810 (2009).

- [9] M. J. Puska and R. M. Nieminen, *Rev. Mod. Phys.* **66**, 841 (1994).
- [10] S. J. Tao, *J. Chem. Phys.* **56**, 5499 (1972); M. Eldrup, D. Lightbody, and J. N. Sherwood, *Chem. Phys.* **63**, 51 (1981).
- [11] Y. Kita, R. Maezono, M. Tachikawa, M. Towler, and R. J. Needs, *J. Chem. Phys.* **131**, 134310 (2009); **135**, 054108 (2011).
- [12] D. Bressanini, M. Mella, and G. Morosi, *J. Chem. Phys.* **108**, 4756 (1998); **109**, 1716 (1998); **109**, 5931 (1998); M. Mella, G. Morosi, D. Bressanini, and S. Elli, **113**, 6154 (2000).
- [13] R. J. Buenker and H. P. Liebermann, *J. Chem. Phys.* **131**, 114107 (2009).
- [14] K. Varga and Y. Suzuki, *Phys. Rev. C* **52**, 2885 (1995).
- [15] G. G. Ryzhikh, J. Mitroy, and K. Varga, *J. Phys. B: At. Mol. Opt. Phys.* **31**, 3965 (1998).
- [16] J. Mitroy, *Phys. Rev. A* **70**, 024502 (2004).
- [17] J. Mitroy, *J. At. Mol. Sci.* **1**, 275 (2010).
- [18] A. Zubiaga, F. Tuomisto, and M. J. Puska, *Phys. Rev. A* **85**, 052707 (2012).
- [19] J. Y. Zhang and J. Mitroy, *Phys. Rev. A* **78**, 012703 (2008).
- [20] M. W. J. Bromley, J. Mitroy, and G. G. Ryzhikh, *J. Phys. B: At. Mol. Opt. Phys.* **31**, 4449 (1998).
- [21] S. K. Houston and R. J. Drachman, *Phys. Rev. A* **3**, 1335 (1971).
- [22] M. Basu and A. S. Gosh, *Phys. Rev. A* **43**, 4746 (1991).
- [23] M. R. McAlinden, A. A. Kernoghan, and H. R. J. Walters, *J. Phys. B: At. Mol. Opt. Phys.* **30**, 1543 (1997).
- [24] E. Boroński and R. M. Nieminen, *Phys. Rev. B* **34**, 3820 (1986).
- [25] M. J. Puska and R. M. Nieminen, *Phys. Rev. B* **29**, 5382 (1984).
- [26] A. Zubiaga *et al.*, “Single particle effective potentials for Ps,” (2013), in preparation.